

Article

A Genome-Wide Comparative Analysis of *AUX1/LAX*, *PIN*, and *ABCB* Genes Reveals Their Roles in Cucumber Fruit Curving

Ke Lu ^{1,2}, La Zhang ^{1,2}, Lianxue Fan ³, Xiuyan Zhou ³ and Shengnan Li ^{1,2,*}¹ College of Advanced Agriculture and Ecological Environment, Heilongjiang University, Harbin 150080, China² Key Laboratory of Sugar Beet Genetic Breeding, Heilongjiang University, Harbin 150080, China³ Key Laboratory of Biology and Genetic Improvement of Horticultural Crops (Northeast Region), Ministry of Agriculture, College of Horticulture and Landscape Architecture,

Northeast Agricultural University, Harbin 150030, China

* Correspondence: 2020046@hlju.edu.cn

Abstract: Auxin transport is regulated by the *AUX1/LAX*, *PIN*, and *ABCB* gene families, controlling the distribution of auxin and ultimately fruit curving in cucumbers. However, studies on the differential expression of these auxin transporters and their roles in fruit curving are limited. In this study, we identified 36 auxin transporters from cucumber, including CsLAX1–7, CsPIN1–10, and CsABCB1–19. Basic characteristic analysis revealed that all CsLAX proteins were conservative, and a C-terminal NPNTY motif was found in CsPIN1–4/7–10. CsABCB1/5/11/14/17 were categorized as half-size transporters. Phylogenetic analysis revealed a genetic relationship between auxin transporters in *Arabidopsis* and cucumber. Exogenous auxin treatment on fruits and qPCR analysis indicated that differential expression patterns of auxin transporters control cucumber fruit curving. Co-expression analysis indicated that *CsPIN1* and *CsLAX2* were substantially negatively correlated, and they displayed opposite expression patterns in curved fruits. A proposed model suggested that *CsLAX2* transports extracellular auxin to the convex side of the fruit; however, *CsPIN1* inhibits auxin efflux at the same location. This leads to uneven auxin distribution that results in cucumber fruit curving.

Keywords: auxin distribution; auxin transporters; cucumber fruit curving; gene expression

Citation: Lu, K.; Zhang, L.; Fan, L.; Zhou, X.; Li, S. A Genome-Wide Comparative Analysis of *AUX1/LAX*, *PIN*, and *ABCB* Genes Reveals Their Roles in Cucumber Fruit Curving.

Agriculture **2024**, *14*, 657. <https://doi.org/10.3390/agriculture14050657>

Academic Editors:

Jacinta Collado-González and María Carmen Piñero

Received: 2 March 2024

Revised: 16 April 2024

Accepted: 19 April 2024

Published: 24 April 2024



Copyright: © 2024 by the authors. Licensee MDPI, Basel, Switzerland. This article is an open access article distributed under the terms and conditions of the Creative Commons Attribution (CC BY) license (<https://creativecommons.org/licenses/by/4.0/>).

1. Introduction

Asymmetric distribution of auxin is crucial for regulating cell differential growth and controlling tissue curving mechanisms in plants, including phototropism [1], gravitropism [2], and apical hook development [3]. Proteins in the plasma membrane (PM) are responsible for auxin transportation between cells [4]. These proteins belong to the three following separate gene families: auxin resistant (AUX) 1/like AUX1 (LAX) influx carriers, pin-formed (PIN) efflux carriers, and ATP-binding cassette B/multidrug-resistance/P-glycoprotein (ABCB/MDR/PGP) efflux/condition transporters [5]. Polar transport involves the active transportation of auxin molecules in the plant organs, which is influenced by the uneven distribution of AUX1/LAX, PIN, and ABCB proteins [6]. Therefore, comparative analysis of these auxin transporters can help in understanding the potential mechanisms of asymmetric growth in plants.

AUX1/LAX proteins belong to the amino acid/auxin permease family that promotes the absorption and movement of auxin in cells [7]. In *Arabidopsis thaliana*, the protein products of four conservative genes (*AUX1*, *LAX1*, *LAX2*, and *LAX3*) resemble to amino acid transporters. *AtAUX1* and *AtLAX3* exhibit separate functions based on their spatial expression patterns. *AtAUX1* promotes entry of auxin to the inner side of the apical hook, whereas *AtLAX3* removes auxin towards the root [8]. Both *AtAUX1* and *AtLAX2* rely on *AXR4* to transport auxin across the membranes of cells involved in root growth [9]. *AtAUX1* protein exhibits varying expression levels on the PM of the outer integument cells and across the entire endosperm, and it regulates seed size via modulating auxin

distribution [10]. Despite numerous reports on the properties and functions of AUX1/LAX, they are frequently overlooked because of the restricted number of family members.

The *PIN* family members are unevenly distributed on the PM, and their placement dictates the direction of auxin transport [11]. The transporters are classified as typical long *PIN* proteins (*PIN1*–*PIN4* and *PIN7*) and short proteins (*PIN5* and *PIN8*) [12]. The long *PIN* proteins are situated on the PM, whereas the shorter proteins *PIN5* and *PIN8* are found in the endoplasmic reticulum. *PIN6* is present in the PM and endoplasmic reticulum [13]. The five long *PIN* proteins reestablish the uneven auxin distribution in the root tip of *Atpin1/3/4/7* mutants; however, *PIN5* and *PIN6* proteins do not possess this ability [14]. *PIN3*, *PIN4*, and *PIN7* have overlapping roles in apical hook development by regulating auxin asymmetric distribution in epidermal cells [8,15]. *OsPIN1b* is involved in auxin transport to regulate plant morphology and root gravity in rice [16]. Naptalam (NPA) specifically targets *PINs* to inhibit auxin transport, leading to a change in the open conformation of the *PIN1* and *PIN8* protein structures [17,18]. Therefore, comparative analysis of *PINs* contributes to understanding their gene function.

The *ABCB* gene family is the second largest subfamily of the ABC transporters, primarily situated symmetrically on the PM to aid in either the intake or release of auxin [19]. Proteins are categorized as full-size-type transporters or half-size transporters based on the quantity of transmembrane domains (TMDs) and nucleotide binding domains [20]. The distinctive configuration improves the auxin transportation capacity of different *ABCB* proteins [21]. It has been identified that *ABCB1/4/14/19/21* is involved in the polar transport of auxin [11]. *AtABCB4*, found in the roots, controls the transport of auxin from the root apex to the epidermis toward the shoot and restricts the elongation of root hair by regulating the efflux of auxin [22,23]. GFP-*ABCB19* is mostly found on the inner side of the hook, and the suppression of hypocotyl elongation by phytochrome is due to decreased *ABCB19*-dependent auxin transport [24,25]. *AtABCB6* and *AtABCB20* controlled the growth of shoots and roots [26,27]. *ABCB15–18* and *ABCB22* participate in the transport of auxin from the lateral root cap and epidermis toward the shoot [28].

Fruit curvature of cucumber (*Cucumis sativus* L.) directly impacts appearance quality and leads to economic losses for farmers. Auxin transport regulates fruit curving via unequal distribution of auxin [29]. However, the potential interactions of auxin transporters in cucumber are unknown. In this study, we aimed to comparatively analyze the gene structure, conserved domains, and *cis*-regulatory elements in the promoter regions of *AUX1/LAX*, *PIN*, and *ABCB* family genes in cucumber. Furthermore, the co-expression network and gene expression analysis were performed to explore the role of auxin transporters in cucumber fruit curving. This study provided a basis for studying the regulation of auxin transport in cucumber fruit curving.

2. Materials and Methods

2.1. Plant Materials and Treatment

The seeds of “changchunmici” cucumber with a fruit curving ratio of 52.56 were grown under 16 h light (at 29 °C)/8 h dark (at 17 °C) conditions in a greenhouse at Northeast Agricultural University, China. The exocarps from curved and straight fruits were collected at 2, 4, 6, 8, and 10 days post-anthesis (DPA) for RT-qPCR analysis.

Experiments with exogenous hormones on cucumber ovaries were performed at 0 DPA. On one side of the ovaries of straight fruits, 30 µM of synthesized indole-3-acetic acid (IAA), 50 µM of efflux inhibitor N-1-naphthylphthalamic acid (NPA), and 0.1 µM of influx inhibitor 2-naphthoxyacetic acid (NOA) were sprayed [30]. For the curved fruits, the three following treatments were set: spraying 30 µM IAA on the concave side, 50 µM NPA on the convex side, or 0.1 µM NOA on the convex side. The fruits treated by ddH₂O were set as the control. The exocarps were collected at 4 DPA to determine auxin content and extract RNA. Three independent biological replicates were set for each treatment. Auxin was extracted as per the method described by Weiler [31], and its concentration was determined using a Plant IAA ELISA kit (Meimian Industrial Co., Ltd., Yancheng, Jiangsu,

China). Statistical analysis was performed using one-way ANOVA. p value < 0.05 was considered significant.

2.2. Characterization and Phylogenetic Analysis of Auxin Transporters

To identify the auxin transporters in cucumber, the v2 whole genome protein sequences of cucumber were obtained from the Cucurbit Genome Database (CuGenDB, <http://cucurbitgenomics.org/>, accessed on 22 August 2023). The Hidden Markov Models (HMM) profiles were analyzed to identify the potential auxin transporters in cucumber, including AUX1/LAX (Pfam 01490), PIN (Pfam 03574), and ABCB (Pfam 00005 and Pfam 00664). Additionally, the protein sequences of *Arabidopsis* auxin transporter from TAIR (<https://www.arabidopsis.org/>, accessed on 22 August 2023) were used as queries in BLASTp searches against the cucumber genome (Table S1), with an e-value of $\leq 10^{-5}$ and bit scores of > 100 . Further, redundant protein sequences were eliminated using the InterPro database (<https://www.ebi.ac.uk/interpro/>, accessed on 22 August 2023) and SMART (<http://smart.embl-heidelberg.de/>, accessed on 22 August 2023).

Protein length (aa), molecular weight (kDa), and isoelectric point (pI) were calculated using Pepstats (https://www.ebi.ac.uk/Tools/seqstats/emboss_pepstats/, accessed on 30 August 2023). The WoLF PSORT program was used to predict the subcellular localization of proteins (<https://wolfpsort.hgc.jp/>, accessed on 18 September 2023) [32]. Multiple sequence alignment analysis was performed using the MUSCLE program, with a gap open value of -2.90 and a gap extension value of 0.00 . A phylogenetic tree was constructed in MEGA 11.0 using the neighbor-joining (NJ) tree method with 1000 replicate bootstraps [33] and was visualized using Evolview v2 [34].

2.3. Gene Structure, Genome Distribution, and Duplication Analysis

Conserved motifs of AUX1/LAX, PIN, and ABCB proteins in cucumber were explored using MEME online software version 5.5.4 (<https://meme-suite.org/meme/doc/meme.html>, accessed on 27 September 2023) and visualized using TBtools version 2.069 [35,36]. The gene structures of the *AUX1/LAX*, *PIN*, and *ABCB* gene families were predicted using TBtools version 2.069 [31]. The TMDs were analyzed using DeepTMHMM version 1.0.24 (<https://dtu.biolib.com/DeepTMHMM>, accessed on 18 September 2023) [37].

The duplicate gene datasets were obtained from Plant Repeat Gene Database (<http://pdgd.njau.edu.cn:8080/>, accessed on 19 February 2023), including whole genome duplications (WGD), tandem duplications, transposed duplications (TRD), dispersed duplications (DSD), and proximal duplication (PD). The collinear blocks between cucumber and *Arabidopsis* were analyzed using MCScanX, with the default parameters of TBtools version 2.069 [38]. The gene duplication and synteny were visualized using TBtools version 2.069 [36].

2.4. Analysis of Cis-Acting Elements of Auxin Transporters

The upstream regions (1500 bp) before the initiation codon (ATG) of the *AUX1/LAX*, *PIN*, and *ABCB* genes of cucumber were obtained from cucumber genome database using TBtools software version 2.069 [36]. These promoter sequences were updated on the PlantCARE website (<https://bioinformatics.psb.ugent.be/webtools/plantcare/html/>, accessed on 27 March 2024) for searching *cis*-acting elements. The enrichment of *cis*-acting elements was analyzed using tidyverse tool and ggplot2 tool in R v4.2.1.

2.5. Co-Expression Analysis of Auxin Transporters

The published transcriptome data by Wang et al. [39] was obtained from the Sequence Read Archive database (accession number: SRP111902), which related to the curved and straight fruits of cucumber at 2 DPA. The transcription factors (TFs) were screened from the above transcriptome data using the PlanTFDB database (<http://plantfdb.cbi.pku.edu.cn/>, accessed on 30 October 2023). The Pearson correlations between TFs and auxin transporters were calculated using the corrplot tool in R v4.2.1, using readings per kilobase

pair per million reads (RPKM > 1). Further, the gene pairs with an absolute correlation coefficient > 0.97 were used to construct co-expression networks. Cytoscape software version 3.10.1 was used for the visualization [40].

2.6. Real-Time Quantitative PCR(RT-qPCR) Analysis

Total RNA was extracted from the exocarps at 2, 4, 6, 8, and 10 DPA using RNA-easy Isolation Reagent (Vazyme, Nanjing, China). The first strand of cDNA was synthesized using the Prime Script™ RT reagent Kit with gDNA Eraser (Takara, Shiga, Japan). RT-qPCR analysis was conducted in the Quantagene q225 system (KUBO, Beijing, China) using TB Green Premix (Takara, Shiga, Japan). The amplification program was set as follows: preheating at 95.0 °C for 30 s, followed by 40 cycles of 95 °C for 5 s and 60 °C for 35 s. The specific primers are given in Table S2. Relative gene expression was determined using the $2^{-\Delta\Delta CT}$ method. Elongation factor 1 alpha (*CsEF1 α*) served as the reference gene [29]. Gene expression levels were visualized with clustering heatmaps using TBtools software (version 2.069) [36]. All experiments were conducted with three biological replicates.

3. Results

3.1. Auxin Transport Contributed to Asymmetric Auxin Distribution and Resulted in Curved Fruit

To determine the impact of auxin transport on fruit curvature, we sprayed exogenous auxin (IAA) and auxin transport inhibitors (NOA and NPA) on both straight and curved fruits. Phenotype analysis revealed that spraying IAA, NPA, and NOA on one side of the ovary of straight fruits (0 DPA) led to formation of curved shape at 4 DPA, whereas IAA treatment on the concave side of the ovary of curved fruits led to the development of straight fruit. When NOA and NPA were sprayed on the convex side of the ovaries of curved fruits, straight fruits were produced at 4 DPA (Figure 1a). Further analysis revealed that auxin content was consistent on both sides of the straight fruits, whereas it was higher on the convex side than on the concave side in curved fruits (Figure 1b). Regardless of the total amount of auxin, any unequal distribution of auxin led to fruit curving (Figure 1c–e). These results revealed that auxin transport contributes to the uneven distribution of auxin in cucumber fruit, resulting in fruit curving.

3.2. Genome-Wide Identification of Auxin Transporters

Auxin-transport-related genes, including seven *LAX*, 10 *PIN*, and 19 *ABCB* genes, were identified in cucumber and named according to their location on the chromosomes (*CsLAX1–7*, *CsPIN1–10*, and *CsABCB1–19*). The sizes of *CsLAX* proteins ranged from 466 to 494 amino acids (aa), with molecular weights ranging from 52.51 to 55.54 kDa and predicted isoelectric points (pIs) ranging from 8.2269 to 9.3645. For *CsPIN* proteins, protein size ranged from 103 to 645 aa, molecular weights ranged from 10.98 to 70.79 kDa, and the estimated pIs ranged from 4.5119 to 10.0279. For *CsABCBs*, molecular weights ranged from 34.39 to 160.12 kDa, pIs ranged from 6.1173 to 9.7729, and protein size ranged from 305 to 1464 aa. *CsPIN4* was predicted to be present in the vacuolar membrane, *CsPIN6*, *CsABCB5*, and *CsABCB17* were predicted to be present in the chloroplast and the others in the PM. All *CsLAX* proteins have 11 transmembrane helices. Except for *CsPIN5* and *CsPIN6*, most *CsPIN* have 10 transmembrane helices. TMD for *CsABCB* proteins ranged from 3 to 14 (Table S3).

3.3. Distribution and Duplication Analysis of Auxin Transporters

In total, 36 auxin transporters were irregularly distributed on seven chromosomes in cucumber. *CsLAXs* were identified on all chromosomes except chromosome 1. *CsPINs* were found on chromosomes 1, 2, 3, 4, and 5. No *CsABCB* gene was found on chromosome 4. The following four types of duplications were found in cucumber: five pairs of WGD, seven pairs of DNA-TRD, 29 pairs of DSD, and one pair of PD (Figure 2). The *CsLAX* genes

were copied 40% via WGD and 60% via scattered duplication. DNA-TRD and DSD were significant factors in the evolution of the *CsPIN* and *CsABCB* families.

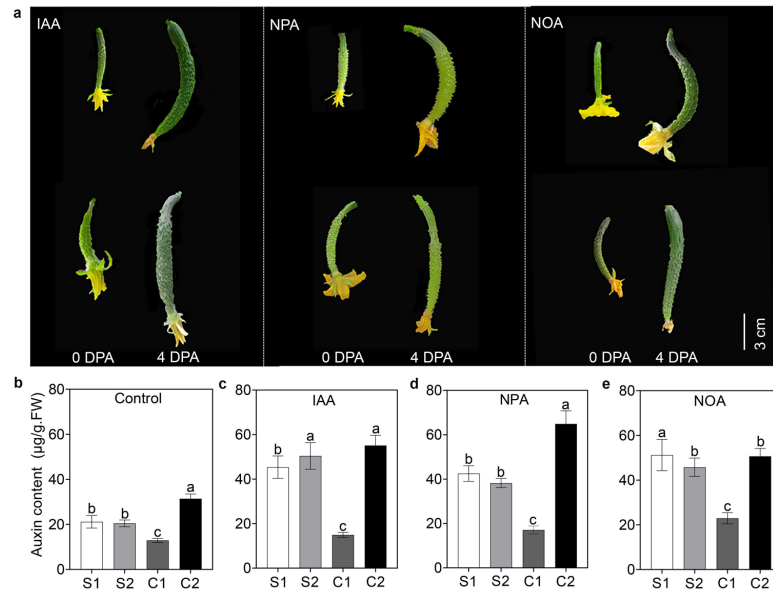


Figure 1. Effects of exogenous auxin treatment on cucumber fruits. (a) Exogenous auxin application on the straight and curved fruits at 0 DPA. Auxin content in the (b) control, (c) IAA treatment, (d) NPA treatment, and (e) NOA treatment at 4 DPA. S1 and S2 represent both sides of the straight fruits; C1 and C2 represent concave and convex sides of the curved fruits, respectively. Scale bar = 3 cm. Data represent the average of three replicates with standard errors. Different letters indicate significant differences ($p < 0.05$).

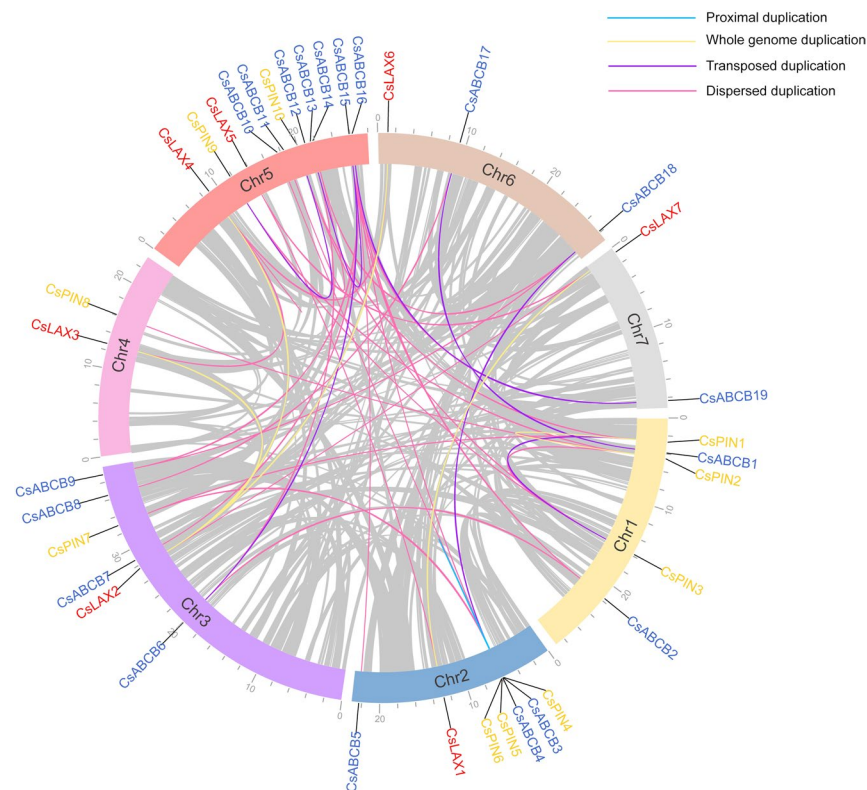


Figure 2. Chromosome localization and distribution of duplication events of *CsLAXs*, *CsPINs*, and *CsABCBs*.

In synteny analysis (Figure 3d), 20 orthologous gene pairs were identified among the three auxin transporter families of cucumber and *Arabidopsis*. Among them, eight pairs of syntenic orthologous genes (one-to-one) were identified, such as *AtLAX3*–*CsLAX5*, *AtPIN2*–*CsPIN3*, and *AtABCB1*–*CsABCB7*. These gene pairs might be derived from a common ancestor. Three *AtLAXs* and one *AtPIN* had a one-to-two corresponding relationship with *CsLAXs* and *CsPINs*, respectively. Two pairs were two *AtABCB* genes corresponding to the same *CsABCB*, such as *AtABCB7* and *AtABCB9*–*CsABCB18*.

Each *CsLAX* protein contained 10 motifs because of the 80.8% sequence similarity (Figure 4). *CsPIN1*–*4*/*7*–*10* had the C-terminal NPNTY motif, known as motif 8, which is a conserved area in the HL domain of the PINs. *CsABCB1*, 5, 11, 14, and 17 had three–eight motifs and were categorized as half-size transporters (Table S4). The *CsLAX* genes had seven to eight exons. The number of exons in *CsPINs* varied between five and seven, except for *CsPIN5* and *CsPIN6*. Subfamily I exhibited a more conservative gene structure compared with subfamily II. The exon–intron architecture exhibited considerable differences, with the number of exons varying from two to 18. The introns of *CsABCB11*, *CsABCB14*, and *CsABCB17* were more in number than those of other subfamily members.

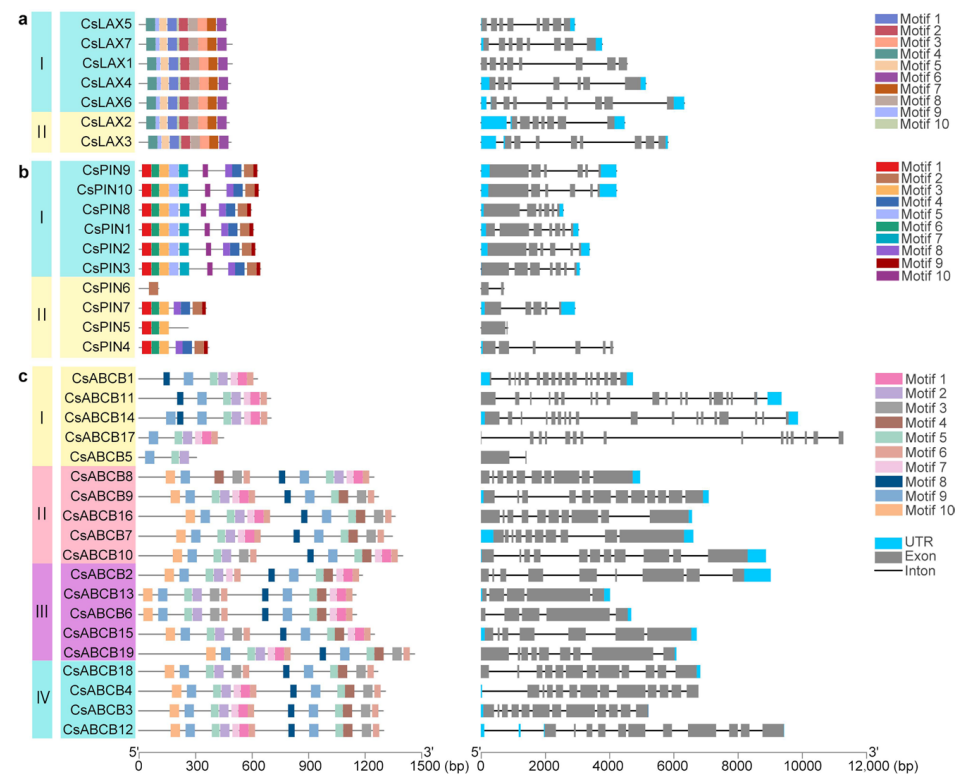


Figure 4. The motif and gene structure of *CsLAXs* (a), *CsPINs* (b), and *CsABCBs* (c).

3.5. Analysis of Cis-Regulatory Elements in the Promoter Regions of Auxin Transporters

A total of 845 *cis*-regulatory elements were obtained in the promoter regions (1500 bp) of auxin transporters. Based on their biological functions, these *cis*-regulatory elements were divided into the following five functional groups: plant growth and development, light response, plant hormone, stress response, and TFs (Figure 5). Particularly, 48 auxin *cis*-regulatory elements, such as AuxRR-core, as-1, TGA-box, and TGA-element, were identified from auxin transporters and were essential for auxin signaling and transport. The TGA-element is known to be an auxin-responsive element, whereas the TGA-box is a part of the auxin-responsive element. Furthermore, most auxin transporters had both MYB- and MYC-responsive regions, suggesting that MYB and MYC TFs may regulate the expression of these genes.

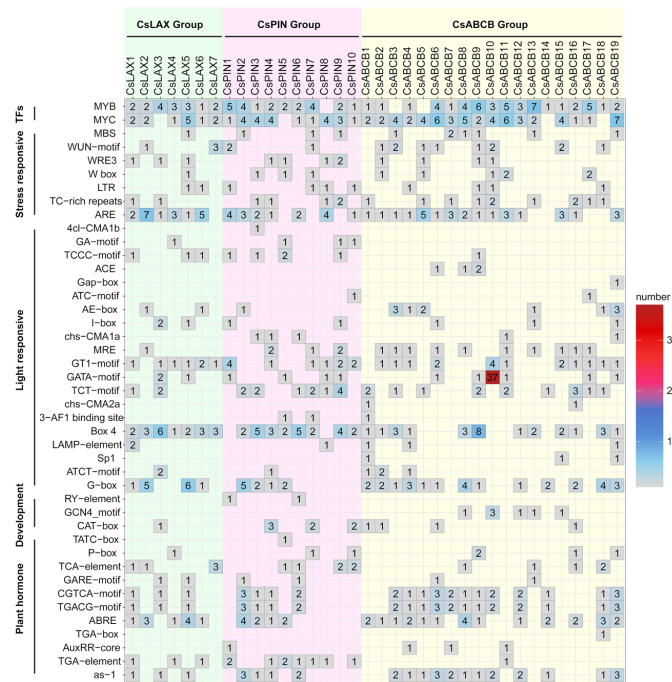


Figure 5. The prediction of cis-regulatory elements in the promoters of auxin transporters.

3.6. Differential Expression of Auxin Transporters Control Fruit Curving

Using qPCR data, a gene expression heatmap was constructed to investigate the role of auxin transporters. The criteria for selecting differentially expressed genes were mean >1 and minimum absolute fold change $|\log_2FC| > 1$. Expression patterns of auxin transporters were different between straight and curved fruits. Curved fruits were produced after IAA treatment, which led to increased expression of *CsLAX2–7*, *CsPIN1–2/7/10*, and *CsABCB1/3/5–7/13/17* on the convex side. However, expressions of these genes were not different on both sides of straight fruits (Figure 6a). *LAX1/2/5*, *PIN1–2/8–10*, and *ABCB2–4/8/11–13/16/19* were differentially expressed on the concave and convex sides of curved fruits, whereas their expressions were similar on both sides of straight fruits (Figure 6b). These results indicated that differential expression patterns of auxin transporters control fruit curving. Clustering analysis further revealed that *CsPIN1–2/9–10* and *CsABCB6–7/9–12/14–17* were grouped together (Figure 6b), indicating they have similar functions in fruit curving.

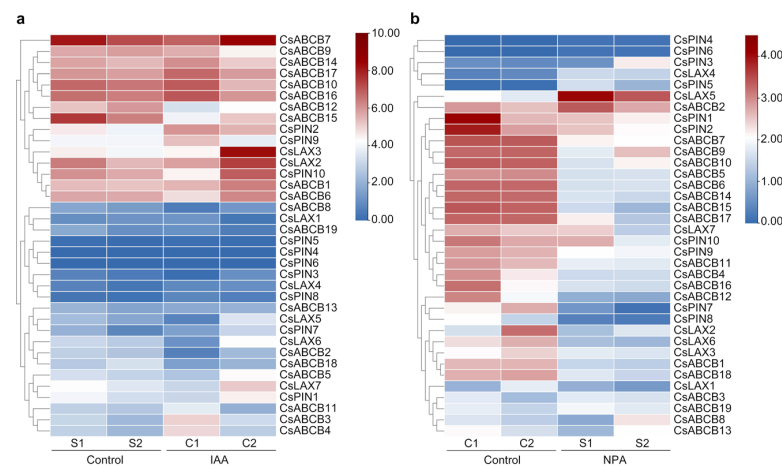


Figure 6. Expression patterns and clustering analysis of auxin transporters under (a) IAA treatment and (b) NPA treatment. S1 and S2 represent both sides of the straight fruits; C1 and C2 represent the concave and convex sides of curved fruits, respectively.

3.7. Potential Roles of Auxin Transporters in Fruit Curving

Based on the published transcriptome data by Wang et al. [39], a co-expression network was constructed using the expression levels of auxin transporters. A total of 14 auxin transporters were significantly correlated with the six guide genes, including *CsLAX1* (its expression level was the same as that of *CsLAX2* reported by Li et al. [29]) (1), *CsLAX2* (2), *CsPIN1* (1), *CsABCB12* (4), *CsABCB16* (4), and *CsABCB18* (2) (Figure 7a and Table S5). Among them, *CsPIN3* was negatively correlated with both *CsABCB12* ($r = -0.999$) and *CsABCB16* ($r = -0.994$), whereas *CsPIN10* was positively correlated with *CsABCB16* ($r = 0.992$) and *CsABCB18* ($r = 0.999$). *CsPIN1* was significantly negatively correlated with *CsLAX2* ($r = -0.999$), indicating that they might play opposite roles in fruit curving. Furthermore, *CsLAX2* and *CsPIN1* exhibited opposite expression patterns, particularly in the concave and convex sides of curved fruits at 4 DPA (Figure 7b). This result was supported by the phenotype of fruits after exogenous auxin treatment. Additionally, during fruit curving, the expression pattern of *CsPIN1* was opposite to that of *CsABCB16* and *CsABCB18*.

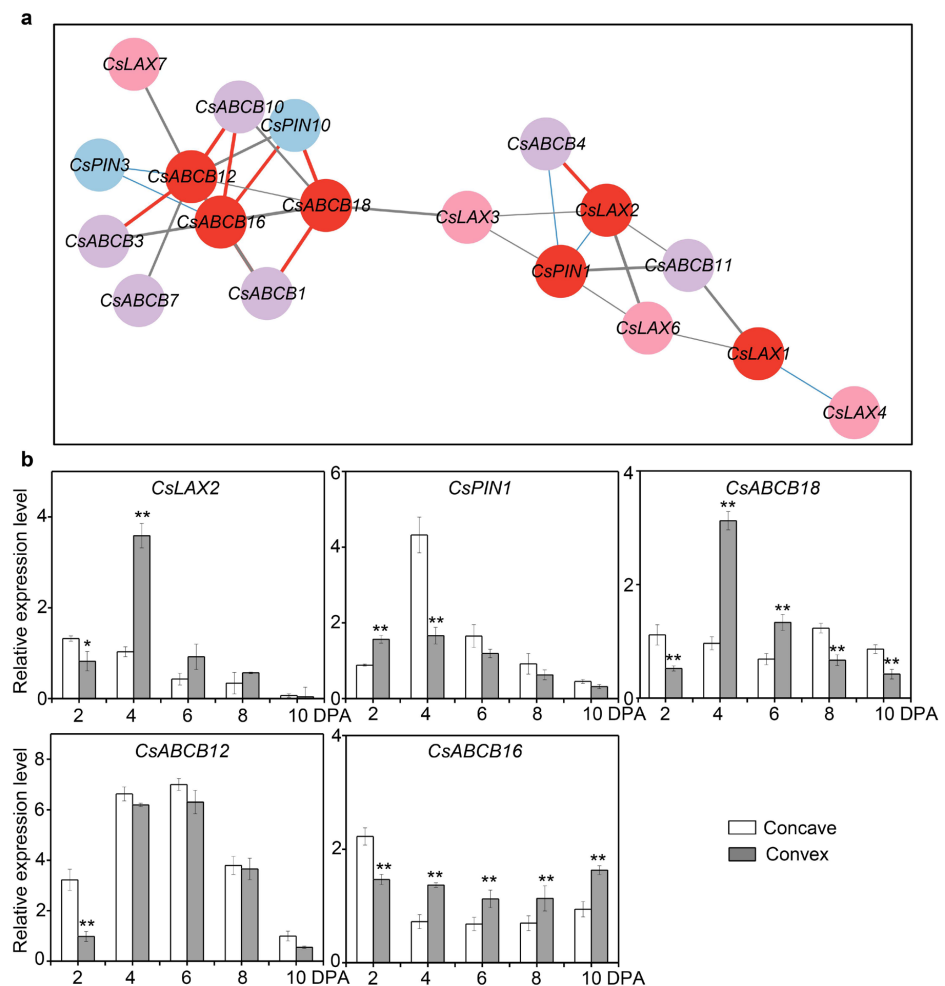


Figure 7. Co-expression network and expression profiles. (a) The co-expression network of LAXs, PINs, and ABCBs on the concave and convex sides of curved cucumber fruits at 2 DPA was established when the Pearson correlation was higher than 0.97 or lower than -0.97 . Different colored circles represent different auxin transport gene families. Red and blue lines show that the Pearson correlation was higher than 0.99 and lower than -0.99 , respectively. (b) The mRNA levels on the concave and convex sides of curved fruits at 2, 4, 6, 8, and 10 DPA. *CsEF1a* was used as the reference gene. The data are the means (\pm SEs) of three independent experiments, with three replicates each (* $p < 0.05$, and ** $p < 0.01$).

3.8. Co-Expression Analysis of TFs and Transporters

In total, 296 TFs were obtained from the published transcriptome data, among which the most abundant TFs were *MYB*, *WRKY*, *NAC*, and *ARF*. A co-expression network was constructed using TFs and guide genes. In the *LAX* group, five TFs, including *ARF* (3) and *MYB* (2) ($r > 0.99$), were strongly correlated with *CsLAX1*; however, 10 TFs were positively correlated with *CsLAX2* (Figure 8a). *MYB* TFs were significantly correlated with *CsPIN1* (Figure 8b). For the *ABCB* group, 13 TFs were typically related to *CsABCB12/16/18* (Figure 8c). These TFs might regulate auxin transporters in fruit curving.

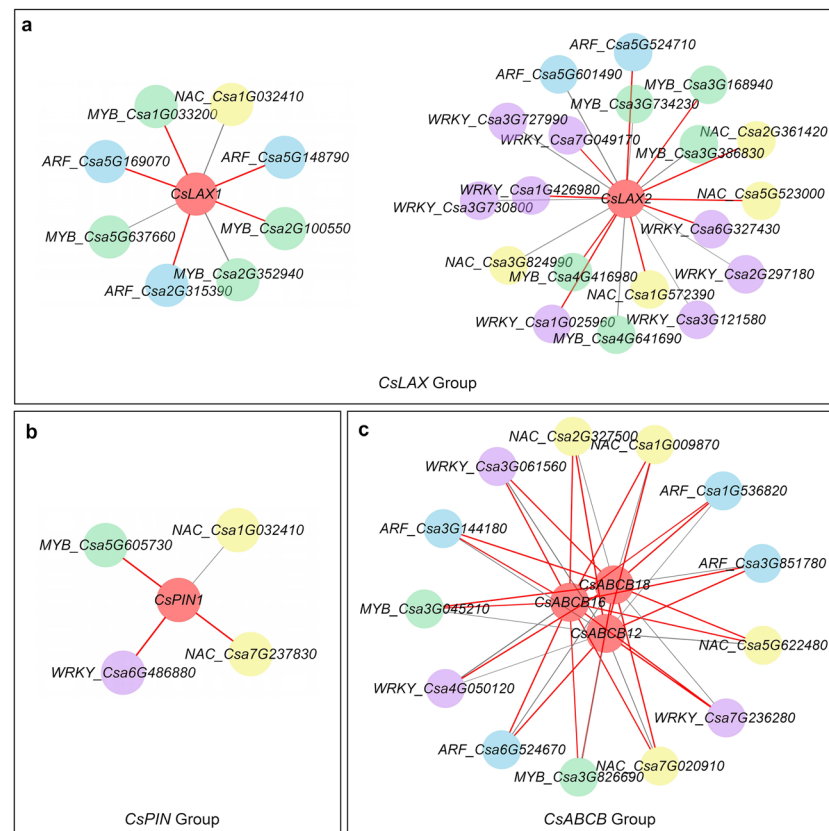


Figure 8. Co-expression network of TFs and guide genes in *CsLAX* (a), *CsPIN* (b) and *CsABCB* (c) group at 2 DPA. The co-expression relationship was established when the Pearson correlation was higher than 0.97. Different colored circles represent different TFs. Red lines indicate that the Pearson correlation was higher than 0.99.

4. Discussion

4.1. Comprehensive Analysis of Auxin Transporters

The analysis of gene structure and motifs contributed to the elucidation of gene function. The results revealed that *CsLAX*s, like *AtLAX*s, had a highly conserved motif and gene structure and consisted of 11 transmembrane helices [13]. The *PIN* protein in *Arabidopsis* contained two closely conserved transmembrane helices at the N and C termini, linked by a cytoplasmic loop in the center [41]. Transmembrane domain analysis revealed that *CsPIN4* and *CsPIN7* had short central hydrophilic loops that were clustered with *AtPIN5* and *AtPIN8*, whereas *CsPIN1–3* and *CsPIN8–10* had long central hydrophilic loops. Previous studies have reported the essential function of the NPNTY motif in facilitating interactions between membrane proteins and receptor proteins [42]. The motif was found to be conserved in cucumber (motif 8), except for *CsPIN5* and *CsPIN6*. *ABCB* proteins were categorized into the following two classes: half- and full-size proteins. The full-size *CcABCBS* in Chinese hickory have a higher number of transmembrane regions than the half-size *CcABCBS* [21]. The same outcome was observed in cucumber (Table S3). These

results suggested that the functions of LAX, PIN, and ABCB proteins were similar in cucumber and *Arabidopsis*.

4.2. Potential Roles of Auxin Transporters

The polar transit of auxin leads to an unequal distribution of AUX/LAX and PIN proteins in cells and tissues. This regulation is essential for conducting the roles of auxin in governing various plant developmental processes [5]. AUX/LAX and PIN proteins typically have contrasting roles in auxin accumulation. *AtAUX1* and *AtPIN2* exhibited opposite expression patterns in regulating auxin levels for root hair elongation under phosphorus stress [43]. Interestingly, *AtAUX1* and *AtPIN2* facilitated the transport of auxin to the root hair meristem for elongation growth in response to low nitrogen stress [44]. *CsPIN1* and *CsPIN7* regulated cucumber fruit length by inhibiting their own expression, leading to decreased auxin levels [45]. The unequal distribution of auxin in the ionospheric zone controlled pedicel abscission in tomatoes by downregulating AUX/LAXs and PINs [46]. AUX/LAX and PIN proteins are involved in plant growth and development, and their impacts can be synergistic or antagonistic.

ABCBs independently play a role in root geotropism, and together with PINs, they control auxin transport. *AtABCB19* interacted with *AtPIN1* by forming homopolymers and heteropolymers to determine auxin transport [47]. Both clustering and co-expression analyses revealed that *CsPIN10* were positively correlated with *CsABCB16* and *CsABCB18* (Figures 6 and 7), indicating their collaborative participation in auxin transport for fruit curving. However, *CsPIN1* and *CsPIN3* were negatively correlated with both *CsABCB12* and *CsABCB16* (Figure 7). *CsPIN1* inhibited the outflow of auxin, whereas *CsABCB16* and *CsABCB18* might promote the export of auxin to rebuild the auxin balance on both sides of the fruit. This result was consistent with a previous study reporting that ABCBs are independently involved in root geotropism, and together with PINs, they regulate auxin transport [48].

The involvement of auxin in plant growth and development is controlled by signal transduction. TFs play a role in binding intracellular and extracellular auxin signals. *ARFs* control the tissue-specific expression of *PIN*, whereas downstream *WRKY23* is involved in regulating auxin feedback on *PIN* polarity localization for root growth [49]. *PtARF7* regulated the expression of *PtPIN1a/b* by binding to the AuxRE motif in their promoter, thereby impacting the feedback mechanism that controls the directional movement of auxin in the cambium of poplar [50]. *AtMYB88* regulated the spatiotemporal expression of *AtPIN3* and *AtPIN7* in root gravitropism [51]. In this study, auxin *cis*-regulatory elements were identified from *PINs* (Figure 5). *MYBs*, *ARFs*, and *WRKYs* might regulate the differential roles of *CsPINs* in fruit curving. The lower expression level of *OsAUX5* was attributed to the weak activation ability of *OsWRKY78* in rice [52]. Decreased expression level of *CsLAX2* on the concave side of fruits may be regulated by *WRKYs* (Figures 7 and 8). Possible interactions between ABCBs and *AtABCB15–18* collaboratively contributed to the development of root structure. *ZmWRKY64* positively controlled the roles of *ZmABCB10/13/32* under cadmium stress [53]. *CsABCB16* expression patterns were consistent with those of *CsABCB18*, suggesting that they have a synergistic impact and are regulated by *WRKYs*. Further studies are essential for exploring the relationship between *WRKYs* and *ABCBs* in cucumber.

4.3. A Model of Fruit Curving in Cucumber

In the apical hook formation in *A. thaliana*, the polar distribution of *PIN3*, *PIN4*, and *PIN7* leads to the transfer of auxin from the central pillar to the epidermal cells outside. *PINs* carry auxin from the outside to the inner side of the hook, whereas *AUX1* on the inner side of the hook facilitate the transfer of auxin into the cell [8,54]. The co-expression network and qPCR analyses (Figure 6) revealed that *CsLAX2* and *CsPIN1* worked together to promote auxin accumulation on the convex side of the curved fruit (Figure 6). The differential expression patterns of *CsLAX2* and *CsPIN1* contributed to the uneven distribution of auxin

on both sides of the fruits (Figures 1 and 6). A hypothetical model indicated that *CsLAX2* was responsible for transporting extracellular auxin to the convex side, whereas *CsPIN1* inhibited the auxin efflux on the convex side. Consequently, unequal distribution of auxin leads to fruit curving.

5. Conclusions

In summary, 36 auxin transporters were identified in cucumber, and the differences in their structure and function were investigated. Exogenous auxin treatment and qPCR results revealed that the polar translocation of auxin led to unequal distribution of AUX1/LAX, PIN, and ABCB proteins. Fruit curvature is attributed to the uneven distribution of auxin controlled by differential expression of *CsLAX2* and *CsPIN1*. This study enhanced the understanding of the basic characteristics of auxin transporters and their roles in cucumber fruit curving.

Supplementary Materials: The following supporting information can be downloaded at: <https://www.mdpi.com/article/10.3390/agriculture14050657/s1>, Table S1: information of LAXs, PINs, and ABCBs from cucumber and *Arabidopsis thaliana*; Table S2: list of specific RT-qPCR primers in this study; Table S3: information on *CsLAX*, *CsPIN*, and *CsABCB* genes and properties of the deduced proteins in cucumber (*Cucumis sativus* L.); Table S4: predicted functional domains of *CsABCBs*; Table S5: co-expression relationship of cucumber LAXs, PINs, and ABCBs.

Author Contributions: Conceptualization, K.L. and S.L.; validation, K.L. and L.Z.; writing—original draft preparation, K.L. and L.Z.; writing—review and editing, K.L., L.F., S.L. and X.Z.; visualization, K.L. and S.L.; project administration, K.L. and S.L. All authors have read and agreed to the published version of the manuscript.

Funding: This research was funded by the National Natural Science Foundation of China grant number 32202475, China Postdoctoral Science Foundation grant number 2021M701127, Natural Science Foundation of Heilongjiang Province grant number YQ2021C032, basic scientific research projects of provincial colleges and universities in Heilongjiang Province grant number 2022-KYYWF-1039.

Institutional Review Board Statement: Not applicable.

Data Availability Statement: All the data supporting the findings of this study are included in this manuscript and Supplementary Materials.

Conflicts of Interest: The authors declare no conflicts of interest.

References

- Hohm, T.; Demarsy, E.; Quan, C.; Allenbach Petrolati, L.; Preuten, T.; Vernoux, T.; Bergmann, S.; Fankhauser, C. Plasma membrane H⁺-ATPase regulation is required for auxin gradient formation preceding phototropic growth. *Mol. Syst. Biol.* **2014**, *10*, 751. [CrossRef] [PubMed]
- Xiao, G.; Zhang, Y. Adaptive growth: Shaping auxin-mediated root system architecture. *Trends Plant Sci.* **2020**, *25*, 121–123. [CrossRef] [PubMed]
- Peng, Y.; Zhang, D.; Qiu, Y.; Xiao, Z.; Ji, Y.; Li, W.; Xia, Y.; Wang, Y.; Guo, H. Growth asymmetry precedes differential auxin response during apical hook initiation in *Arabidopsis*. *J. Integr. Plant Biol.* **2022**, *64*, 5–22. [CrossRef] [PubMed]
- Dindas, J.; Scherzer, S.; Roelfsema, M.R.G.; von Meyer, K.; Müller, H.M.; Al-Rasheid, K.A.S.; Palme, K.; Dietrich, P.; Becker, D.; Bennett, M.J.; et al. AUX1-mediated root hair auxin influx governs SCF^{TIR1/AFB}-type Ca²⁺ signaling. *Nat. Commun.* **2018**, *9*, 1174. [CrossRef] [PubMed]
- Yang, C.; Wang, D.; Zhang, C.; Ye, M.; Kong, N.; Ma, H.; Chen, Q. Comprehensive Analysis and Expression Profiling of PIN, AUX/LAX, and ABCB Auxin Transporter Gene Families in *Solanum tuberosum* under Phytohormone Stimuli and Abiotic Stresses. *Biology* **2021**, *10*, 127. [CrossRef] [PubMed]
- An, F.; Zhang, X.; Zhu, Z.; Ji, Y.; He, W.; Jiang, Z.; Li, M.; Guo, H. Coordinated regulation of apical hook development by gibberellins and ethylene in etiolated *Arabidopsis* seedlings. *Cell Res.* **2012**, *22*, 915–927. [CrossRef] [PubMed]
- Zhao, H.; Maokai, Y.; Cheng, H.; Guo, M.; Liu, Y.; Wang, L.; Chao, S.; Zhang, M.; Lai, L.; Qin, Y. Characterization of auxin transporter *AUX*, *PIN* and *PILS* gene families in pineapple and evaluation of expression profiles during reproductive development and under abiotic stresses. *PeerJ* **2021**, *9*, e11410. [CrossRef]
- Vandenbussche, F.; Petrášek, J.; Žádníková, P.; Hoyerová, K.; Pešek, B.; Raz, V.; Swarup, R.; Bennett, M.; Zažímalová, E.; Benková, E. The auxin influx carriers AUX1 and LAX3 are involved in auxin-ethylene interactions during apical hook development in *Arabidopsis thaliana* seedlings. *Development* **2010**, *137*, 597–606. [CrossRef] [PubMed]

9. Tidy, A.; Abu Bakar, N.; Carrier, D.; Kerr, I.D.; Hodgman, C.; Bennett, M.J.; Swarup, R. Mechanistic insight into the role of AUXIN RESISTANCE4 in trafficking of AUXIN1 and LIKE AUX1-2. *Plant Physiol.* **2024**, *194*, 422–433. [[CrossRef](#)]
10. Liu, H.; Luo, Q.; Tan, C.; Song, J.; Zhang, T.; Men, S. Biosynthesis- and transport-mediated dynamic auxin distribution during seed development controls seed size in Arabidopsis. *Plant J.* **2023**, *113*, 1259–1277. [[CrossRef](#)]
11. Zhang, Y.; Berman, A.; Shani, E. Plant Hormone Transport and Localization: Signaling Molecules on the Move. *Annu. Rev. Plant Biol.* **2023**, *74*, 453–479. [[CrossRef](#)] [[PubMed](#)]
12. Bennett, T.; Brockington, S.F.; Rothfels, C.; Graham, S.W.; Stevenson, D.; Kutchan, T.; Rolf, M.; Thomas, P.; Wong, G.K.-S.; Leyser, O.; et al. Paralogous Radiations of PIN Proteins with Multiple Origins of Noncanonical PIN Structure. *Mol. Biol. Evol.* **2014**, *31*, 2042–2060. [[CrossRef](#)] [[PubMed](#)]
13. Hammes, U.Z.; Murphy, A.S.; Schwechheimer, C. Auxin transporters—A biochemical view. *Cold Spring Harbor Perspect. Biol.* **2022**, *14*, a039875. [[CrossRef](#)] [[PubMed](#)]
14. Zhang, Y.; Rodriguez, L.; Li, L.; Zhang, X.; Friml, J. Functional innovations of PIN auxin transporters mark crucial evolutionary transitions during rise of flowering plants. *Sci. Adv.* **2020**, *6*, eabc8895. [[CrossRef](#)] [[PubMed](#)]
15. Žádníková, P.; Petrášek, J.; Marhavý, P.; Raz, V.; Vandenbussche, F.; Ding, Z.; Schwarzerová, K.; Morita, M.T.; Tasaka, M.; Hejátko, J. Role of PIN-mediated auxin efflux in apical hook development of *Arabidopsis thaliana*. *Development* **2010**, *137*, 607–617. [[CrossRef](#)]
16. Wang, H.; Ouyang, Q.; Yang, C.; Zhang, Z.; Hou, D.; Liu, H.; Xu, H. Mutation of *OsPIN1b* by CRISPR/Cas9 Reveals a Role for Auxin Transport in Modulating Rice Architecture and Root Gravitropism. *Int. J. Mol. Sci.* **2022**, *23*, 8965. [[CrossRef](#)] [[PubMed](#)]
17. Ung, K.L.; Winkler, M.; Schulz, L.; Kolb, M.; Janacek, D.P.; Dedic, E.; Stokes, D.L.; Hammes, U.Z.; Pedersen, B.P. Structures and mechanism of the plant PIN-FORMED auxin transporter. *Nature* **2022**, *609*, 605–610. [[CrossRef](#)] [[PubMed](#)]
18. Yang, Z.; Xia, J.; Hong, J.; Zhang, C.; Wei, H.; Ying, W.; Sun, C.; Sun, L.; Mao, Y.; Gao, Y.; et al. Structural insights into auxin recognition and efflux by *Arabidopsis* PIN1. *Nature* **2022**, *609*, 611–615. [[CrossRef](#)] [[PubMed](#)]
19. Geisler, M.; Aryal, B.; Di Donato, M.; Hao, P. A critical view on ABC transporters and their interacting partners in auxin transport. *Plant Cell Physiol.* **2017**, *58*, 1601–1614. [[CrossRef](#)]
20. Que, F.; Zhu, Y.; Liu, Q.; Wei, Q.; Ramakrishnan, M. Genome-Wide Identification, Expansion, Evolution, and Expression Analysis Reveals ABCB Genes Important for Secondary Cell Wall Development in Moso Bamboo (*Phyllostachys edulis*). *Agronomy* **2023**, *13*, 1828. [[CrossRef](#)]
21. Yang, Y.; Huang, Q.; Wang, X.; Mei, J.; Sharma, A.; Tripathi, D.K.; Yuan, H.; Zheng, B. Genome-wide identification and expression profiles of ABCB gene family in Chinese hickory (*Carya cathayensis* Sarg.) during grafting. *Plant Physiol. Biochem.* **2021**, *168*, 477–487. [[CrossRef](#)] [[PubMed](#)]
22. Kubeš, M.; Yang, H.; Richter, G.L.; Cheng, Y.; Młodzińska, E.; Wang, X.; Blakeslee, J.J.; Carraro, N.; Petrášek, J.; Zažímalová, E. The Arabidopsis concentration-dependent influx/efflux transporter ABCB4 regulates cellular auxin levels in the root epidermis. *Plant J.* **2012**, *69*, 640–654. [[CrossRef](#)]
23. Cho, M.; Lee, S.H.; Cho, H.-T. P-Glycoprotein4 displays auxin efflux transporter-like action in *Arabidopsis* root hair cells and tobacco cells. *Plant Cell* **2007**, *19*, 3930–3943. [[CrossRef](#)]
24. Wu, G.; Cameron, J.N.; Ljung, K.; Spalding, E.P. A role for ABCB19-mediated polar auxin transport in seedling photomorphogenesis mediated by cryptochrome 1 and phytochrome B. *Plant J. Cell Mol. Biol.* **2010**, *62*, 179–191. [[CrossRef](#)] [[PubMed](#)]
25. Mazzella, M.A.; Casal, J.J.; Muschietti, J.P.; Fox, A.R. Hormonal networks involved in apical hook development in darkness and their response to light. *Front. Plant Sci.* **2014**, *5*, 52. [[CrossRef](#)]
26. Jenness, M.K.; Tayengwa, R.; Bate, G.A.; Tapken, W.; Zhang, Y.; Pang, C.; Murphy, A.S. Loss of multiple ABCB auxin transporters recapitulates the major twisted dwarf 1 phenotypes in *Arabidopsis thaliana*. *Front. Plant Sci.* **2022**, *13*, 840260. [[CrossRef](#)] [[PubMed](#)]
27. Zhang, Y.; Nasser, V.; Pisanty, O.; Omary, M.; Wulff, N.; Di Donato, M.; Tal, I.; Hauser, F.; Hao, P.; Roth, O. A transportome-scale amiRNA-based screen identifies redundant roles of *Arabidopsis* ABCB6 and ABCB20 in auxin transport. *Nat. Commun.* **2018**, *9*, 4204. [[CrossRef](#)]
28. Chen, J.; Hu, Y.; Hao, P.; Tsering, T.; Xia, J.; Zhang, Y.; Roth, O.; Njo, M.F.; Sterck, L.; Hu, Y. ABCB-mediated shootward auxin transport feeds into the root clock. *EMBO Rep.* **2023**, *24*, e56271. [[CrossRef](#)]
29. Li, S.; Wang, C.; Zhou, X.; Liu, D.; Liu, C.; Luan, J.; Qin, Z.; Xin, M. The curvature of cucumber fruits is associated with spatial variation in auxin accumulation and expression of a YUCCA biosynthesis gene. *Hortic. Res.* **2020**, *7*, 35. [[CrossRef](#)]
30. Jahn, L.; Hofmann, U.; Ludwig-Müller, J. Indole-3-Acetic Acid Is Synthesized by the Endophyte *Cyanodermella asteris* via a Tryptophan-Dependent and -Independent Way and Mediates the Interaction with a Non-Host Plant. *Int. J. Mol. Sci.* **2021**, *22*, 2651. [[CrossRef](#)]
31. Weiler, E.; Jourdan, P.; Conrad, W. Levels of indole-3-acetic acid in intact and decapitated coleoptiles as determined by a specific and highly sensitive solid-phase enzyme immunoassay. *Planta* **1981**, *153*, 561–571. [[CrossRef](#)] [[PubMed](#)]
32. Horton, P.; Park, K.-J.; Obayashi, T.; Fujita, N.; Harada, H.; Adams-Collier, C.; Nakai, K. WoLF PSORT: Protein localization predictor. *Nucleic Acids Res.* **2007**, *35*, W585–W587. [[CrossRef](#)] [[PubMed](#)]
33. Tamura, K.; Stecher, G.; Kumar, S. MEGA11: Molecular evolutionary genetics analysis version 11. *Mol. Biol. Evol.* **2021**, *38*, 3022–3027. [[CrossRef](#)] [[PubMed](#)]
34. He, Z.; Zhang, H.; Gao, S.; Lercher, M.J.; Chen, W.-H.; Hu, S. Evolview v2: An online visualization and management tool for customized and annotated phylogenetic trees. *Nucleic Acids Res.* **2016**, *44*, W236–W241. [[CrossRef](#)] [[PubMed](#)]

35. Bailey, T.L.; Boden, M.; Buske, F.A.; Frith, M.; Grant, C.E.; Clementi, L.; Ren, J.; Li, W.W.; Noble, W.S. MEME SUITE: Tools for motif discovery and searching. *Nucleic Acids Res.* **2009**, *37*, W202–W208. [[CrossRef](#)] [[PubMed](#)]
36. Chen, C.; Wu, Y.; Li, J.; Wang, X.; Zeng, Z.; Xu, J.; Liu, Y.; Feng, J.; Chen, H.; He, Y. TBtools-II: A “one for all, all for one” bioinformatics platform for biological big-data mining. *Mol. Plant* **2023**, *16*, 1733–1742. [[CrossRef](#)] [[PubMed](#)]
37. Hallgren, J.; Tsigirigos, K.D.; Pedersen, M.D.; Almagro Armenteros, J.J.; Marcatili, P.; Nielsen, H.; Krogh, A.; Winther, O. DeepTMHMM predicts alpha and beta transmembrane proteins using deep neural networks. *BioRxiv* **2022**. [[CrossRef](#)]
38. Wang, Y.; Tang, H.; Debarry, J.D.; Tan, X.; Li, J.; Wang, X.; Lee, T.-h.; Jin, H.; Marler, B.; Guo, H. MCScanX: A toolkit for detection and evolutionary analysis of gene synteny and collinearity. *Nucleic Acids Res.* **2012**, *40*, e49. [[CrossRef](#)] [[PubMed](#)]
39. Wang, C.; Xin, M.; Zhou, X.; Liu, C.; Li, S.; Liu, D.; Xu, Y.; Qin, Z. The novel ethylene-responsive factor *CsERF025* affects the development of fruit bending in cucumber. *Plant Mol. Biol.* **2017**, *95*, 519–531. [[CrossRef](#)]
40. Smoot, M.E.; Ono, K.; Ruschinski, J.; Wang, P.-L.; Ideker, T. Cytoscape 2.8: New features for data integration and network visualization. *Bioinformatics* **2011**, *27*, 431–432. [[CrossRef](#)]
41. Li, Y.; Yang, S.; Shi, M.; Zhang, S.; Wu, S.; Chen, Y.; Li, W.; Tian, W.-M. HbARF2 and HbARF16. 3 function as negative regulators for the radial trunk growth of rubber tree. *Ind. Crops Prod.* **2020**, *158*, 112978. [[CrossRef](#)]
42. Gou, H.; Nai, G.; Lu, S.; Ma, W.; Chen, B.; Mao, J. Genome-wide identification and expression analysis of *PIN* gene family under phytohormone and abiotic stresses in *Vitis vinifera* L. *Physiol. Mol. Biol. Plants* **2022**, *28*, 1905–1919. [[CrossRef](#)]
43. Villaécija-Aguilar, J.A.; Körösy, C.; Maisch, L.; Hamon-Josse, M.; Petrich, A.; Magosch, S.; Chapman, P.; Bennett, T.; Gutjahr, C. KAI2 promotes Arabidopsis root hair elongation at low external phosphate by controlling local accumulation of AUX1 and PIN2. *Curr. Biol.* **2022**, *32*, 228–236. e223. [[CrossRef](#)] [[PubMed](#)]
44. Jia, Z.; Giehl, R.F.H.; Hartmann, A.; Estevez, J.M.; Bennett, M.J.; von Wirén, N. A spatially concerted epidermal auxin signaling framework steers the root hair foraging response under low nitrogen. *Curr. Biol.* **2023**, *33*, 3926–3941.e3925. [[CrossRef](#)] [[PubMed](#)]
45. Zhao, J.; Jiang, L.; Che, G.; Pan, Y.; Li, Y.; Hou, Y.; Zhao, W.; Zhong, Y.; Ding, L.; Yan, S. A functional allele of *CsFUL1* regulates fruit length through repressing *CsSUP* and inhibiting auxin transport in cucumber. *Plant Cell* **2019**, *31*, 1289–1307. [[CrossRef](#)]
46. Dong, X.; Ma, C.; Xu, T.; Reid, M.S.; Jiang, C.-Z.; Li, T. Auxin response and transport during induction of pedicel abscission in tomato. *Hortic. Res.* **2021**, *8*, 192. [[CrossRef](#)]
47. Teale, W.D.; Pasternak, T.; Dal Bosco, C.; Dovzhenko, A.; Kratzat, K.; Bildl, W.; Schwörer, M.; Falk, T.; Ruperti, B.; V Schaefer, J.; et al. Flavonol-mediated stabilization of PIN efflux complexes regulates polar auxin transport. *EMBO J.* **2021**, *40*, e104416. [[CrossRef](#)]
48. Mellor, N.L.; Voß, U.; Ware, A.; Janes, G.; Barrack, D.; Bishopp, A.; Bennett, M.J.; Geisler, M.; Wells, D.M.; Band, L.R. Systems approaches reveal that ABCB and PIN proteins mediate co-dependent auxin efflux. *Plant Cell* **2022**, *34*, 2309–2327. [[CrossRef](#)]
49. Hajný, J.; Tan, S.; Friml, J. Auxin canalization: From speculative models toward molecular players. *Curr. Opin. Plant Biol.* **2022**, *65*, 102174. [[CrossRef](#)]
50. Hu, J.; Su, H.; Cao, H.; Wei, H.; Fu, X.; Jiang, X.; Song, Q.; He, X.; Xu, C.; Luo, K. AUXIN RESPONSE FACTOR7 integrates gibberellin and auxin signaling via interactions between DELLA and AUX/IAA proteins to regulate cambial activity in poplar. *Plant Cell* **2022**, *34*, 2688–2707. [[CrossRef](#)]
51. Wang, H.-Z.; Yang, K.-Z.; Zou, J.-J.; Zhu, L.-L.; Xie, Z.D.; Morita, M.T.; Tasaka, M.; Friml, J.; Grotewold, E.; Beeckman, T. Transcriptional regulation of *PIN* genes by FOUR LIPS and MYB88 during *Arabidopsis* root gravitropism. *Nat. Commun.* **2015**, *6*, 8822. [[CrossRef](#)] [[PubMed](#)]
52. Shi, Y.; Zhang, Y.; Sun, Y.; Xie, Z.; Luo, Y.; Long, Q.; Feng, J.; Liu, X.; Wang, B.; He, D. Natural variations of *OsAUX5*, a target gene of *OsWRKY78*, control the neutral essential amino acid content in rice grains. *Mol. Plant* **2023**, *16*, 322–336. [[CrossRef](#)] [[PubMed](#)]
53. Gu, L.; Hou, Y.; Sun, Y.; Chen, X.; Wang, G.; Wang, H.; Zhu, B.; Du, X. The maize WRKY transcription factor *ZmWRKY64* confers cadmium tolerance in Arabidopsis and maize (*Zea mays* L.). *Plant Cell Rep.* **2024**, *43*, 44. [[CrossRef](#)]
54. Béziat, C.; Barbez, E.; Feraru, M.I.; Lucyshyn, D.; Kleine-Vehn, J. Light triggers PILS-dependent reduction in nuclear auxin signalling for growth transition. *Nat. Plants* **2017**, *3*, 17105. [[CrossRef](#)]

Disclaimer/Publisher’s Note: The statements, opinions and data contained in all publications are solely those of the individual author(s) and contributor(s) and not of MDPI and/or the editor(s). MDPI and/or the editor(s) disclaim responsibility for any injury to people or property resulting from any ideas, methods, instructions or products referred to in the content.